Proceedings of ASME FEDSM'03
4th ASME_JSME Joint Fluids Engineering Conference
Honolulu, Hawaii, USA, July 6-10, 2003

FEDSM2003-45024

WAVELET ANALYSIS OF SPACE-VARYING INTERMITTENT WALL PRESSURE FIELD OF TRANSITIONAL BOUNDARY LAYER

Stephen R. Snarski
Naval Undersea Warfare Center
Newport, RI

ABSTRACT

Measurements of the space-time fluctuating wall pressure field across the transition region of a flat plate zero pressure gradient boundary layer have been performed in an anechoic wind tunnel with a 64-element linear array of sub-miniature hearing-aid microphones (d^+ = 15). Wavelet transforms are being used to quantify the structure and nonhomogeneous wavenumber-frequency spectral content of the field. The results illustrate that the fluctuations *within the turbulent spots* scale with those which exists in a fully developed turbulent boundary layer consistent with previous findings. The spectral contributions due to a second much larger length/time scale associated with the mean *spacing between spots* (e.g., turbulent spot wavepacket pulse trains) is under investigation. Based on an analysis of sinusoidal pulse train signals and consideration of the well established bursting frequency in turbulent boundary layers, it is conjectured here that the turbulent spot wavepacket pulse trains should produce a statistical distribution of energy about the mean fundamental pulse train frequency.

INTRODUCTION

This paper discusses the use of wavelet transform based methods to describe an intermittent and nonhomogeneous space-time field; namely, the wall pressure field beneath a transitional boundary layer. Details of the experiments as well as the results of some preliminary data analysis were presented in Snarski[1]. The objective here is to use wavelet transforms to more appropriately characterize the intermittent space-varying structure of the transitional wall pressure field and the form of the space-varying (nonhomogeneous) wavenumber-frequency spectrum.

The process of transition from a laminar to turbulent boundary layer has been studied extensively in the literature (see recent review in [2]). Initially, the boundary layer flow is laminar in which all the flow variables are steady as shown in Fig. 1. Although the full transition process from stable laminar to fully developed turbulent flow involves three phases of breakdown as illustrated in Fig. 1, only the last stage of transition involving the formation and growth of turbulent spots is of interest here since this is the first place where instantaneous pressure fluctuations are large enough to be of much engineering consequence. Within this region, turbulent spots emerge randomly in space and time at local regions of high shear and subsequently grow in spatial extent as they convect downstream until they eventually coalesce forming the fully developed equilibrium turbulent boundary layer (TBL). This region, referred to herein as the transitional boundary layer or XBL (i.e., x-dependent boundary layer) is typically characterized by the intermittency level $0 < \gamma(x) < 1$ which is a montonically increasing function that defines the fraction of time in which the field is turbulent. This is also the region in which the mean velocity profile $U(y)$ changes from the Blasius to turbulent profiles.

The key point to take away from Fig. 1 is that unlike the TBL in which the average structure of the field is both continuous and independent of time and space (statistically stationary and homogeneous), the XBL field is discontinuous (intermittent) and evolves spatially, quite strongly as a matter of fact, with the downstream coordinate x (streamwise nonhomogeneous). Although some experimental [3-6] and modeling [6-8] work has been done to characterize the space-varying field statistics, the current understanding is incomplete due to limitations in the experimental methods and modeling assumptions (see [1]). A perhaps larger limitation, however, is that all of the previous investigations have relied exclusively on the use of Fourier Transform based methods, best suited for continuous and stationary/homogeneous processes, to describe the intermittent and nonhomogeneous space-time field.

In the present paper, wavelet transforms are used to interrogate a highly resolved space-time transitional wall pressure field data base to provide a better understanding of the structure and spectral content of the XBL wall pressure field.

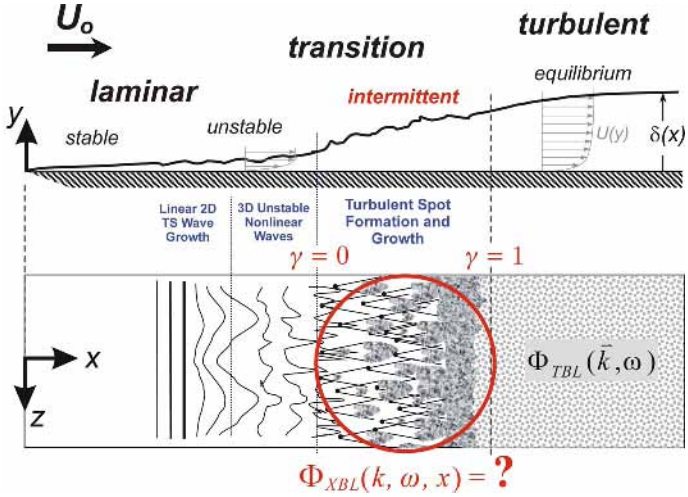

Figure 1. Laminar-to-turbulent boundary layer transition process on a flat plate.

NOMENCLATURE

C_f	Coefficient of local skin friction, $C_f = \tau_w/(\frac{1}{2}\rho U_o^2)$
d	Sensor diameter
k_x	Streamwise wavenumber
L, T	Sampling length (array length) and time
t	Time
T_s	Time between pulses (pulse train period)
U_o	Free stream velocity
u_τ	Friction velocity = $(\tau_w/\rho)^{1/2}$
x, y, z	Streamwise, wall-normal, spanwise coordinates
δ, δ^*, θ	Boundary layer, displacement, and momentum thicknesses
$\gamma(x)$	Intermittency
λ_c	Convective wavelength of turbulence, $\lambda_c = 2\pi/k_c$
$\lambda_s(x)$	Turbulent spot pulse train spatial wavelength
ν	Kinematic viscosity
ω	Circular frequency, $\omega = 2\pi f$
ρ	Fluid density
$\Phi_{TBL}(k, \omega)$	Homogenous TBL wavenumber-frequency wall pressure spectrum
$\Phi_{XBL}(k, \omega, x)$	Nonhomogeneous XBL wavenumber-frequency wall pressure spectrum
τ_w	Wall shear stress
TBL	Turbulent boundary layer
XBL	Transitional (x-dependent) boundary layer

EXPERIMENTS

The experiments discussed herein are the wind tunnel measurements reported by Snarski [1] of the space-time fluctuating wall pressure field beneath a flat plate zero-pressure gradient transitional boundary layer using a 64-element linear array of subminiature hearing-aid microphones (Knowles FG-3329). For these measurements, a 1.16 m wide by 2.00 m long flat plate which housed the 0.35 m long array of microphones was suspended vertically in the cylindrical test section of the NUWC Acoustic Wind Tunnel as shown in Fig. 2. Wall pressure data was acquired at 14 free stream velocities in the range from U_o = 3.44 to 9.01 m/s which corresponded to Reynolds numbers of $Re_x = U_o x/\nu$ = 1.52 - 6.09 x 10^5 and $Re_\theta = U_o\theta/\nu$ = 204 – 1116 across the array (free stream turbulence level of 1.2%). The intermittency level of the wall pressure field across the array over this range of flow speeds is shown in Fig. 3. As speed is increased, the transition zone gradually shifted across the array enabling the complete transition zone to be captured in an overlapping segmented fashion. Mean boundary layer velocity profiles at the mid-array position across this range of flow speeds are shown in Fig. 4. The boundary layer clearly shows the expected transition from the Blasius to turbulent profiles. The flow conditions and boundary layer parameters for the measurements are summarized in Table I.

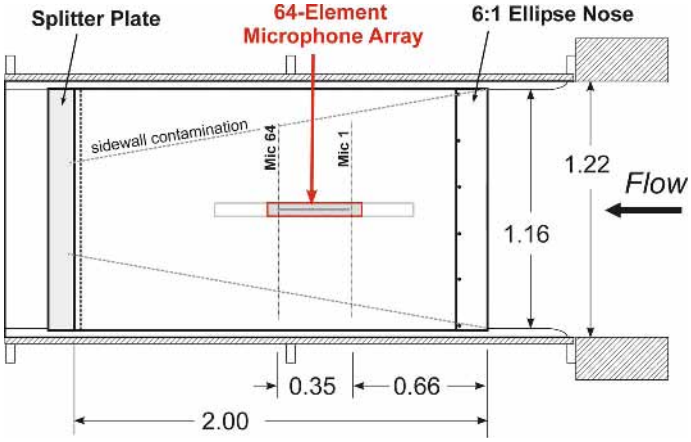

Figure 2. Schematic of Wind Tunnel Measurements (all dimensions in m).

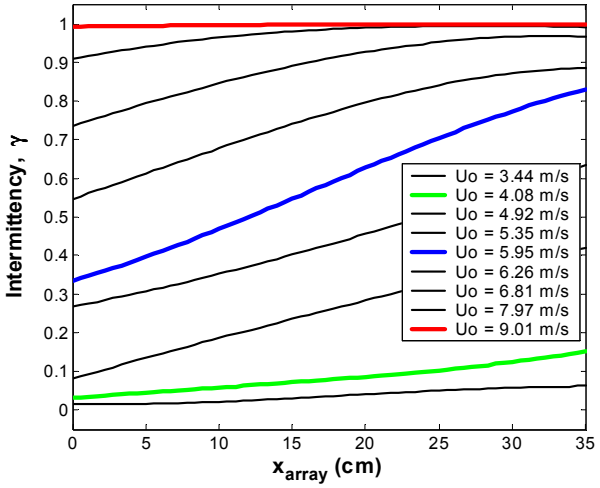

Figure 3. Wall pressure intermittency levels across array over range of flow speeds investigated.

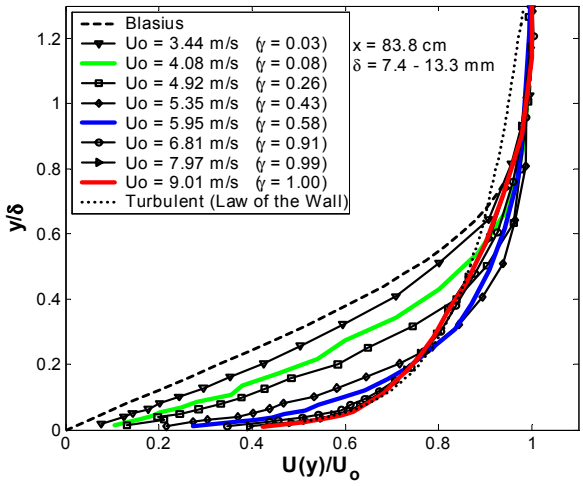

Figure 4. Mean velocity profiles in boundary layer at mid array location over range of flow speeds investigated.

Measurement Conditions	Boundary Layer Parameters
U_o = 3.44 – 9.01m/s	δ = 7.28 – 17.1 mm
x = 66.4 – 101.2 cm	δ^* = 1.53 – 2.55 mm
ρ = 1.2 kg/m^3	$H=\delta^*/\theta$ = 1.37 – 2.27 mm
ν = 15.0 x 10^{-6} m^2/s	$Re_\theta = U_o\theta/\nu$ = 204 – 1116
$Re_x = U_o x/\nu$ = 1.52 – 6.09 x 10^5	γ = 0.01 – 1.00
Resolution Parameters	**Wall Shear Parameters (est.)**
d = 0.76 mm (pinhole)	C_f = 1.8 – 4.8 x 10^{-3}
d/δ^* = 0.30 – 0.50	u_τ = 0.10 – 0.33 m/s
$d^+ = du_\tau/\nu$ = 4.3 – 22.3 (est.)	τ_w = 0.014 – 0.369 Pa

Table I. Flow conditions and measured boundary layer properties across array over range of flow speeds investigated.

RESULTS AND DISCUSSION

Time series data across the entire array associated with the three colored curves in Fig. 3 and 4 are shown in Fig. 5. The time series in Fig. 5 have been digitally high pass filtered at 200 Hz to remove acoustic contamination for purposes of presentation. The variation in intermittency across the array for each speed is indicated to the right of each plot. At U_o = 4.08 m/s, the formation and convection of a single turbulent spot is evident. At U_o = 5.95 m/s many more spots now appear at different stages of their evolution. At U_o = 9.01 m/s, the flow across the entire array is fully turbulent.

Wall pressure frequency autospectra computed using conventional FFT methods for the time signals at microphone 32 (array center) across the full range of flow speeds investigated are shown in Fig. 6. In Fig. 6(a) the spectra are presented in physical variables and show a monotonic increase in spectral levels and frequency distribution as the boundary layer becomes more and more turbulent. In Fig. 6(b), these results are nondimensionalized on boundary layer outer length and velocity scales as well as by the intermittency level γ. In

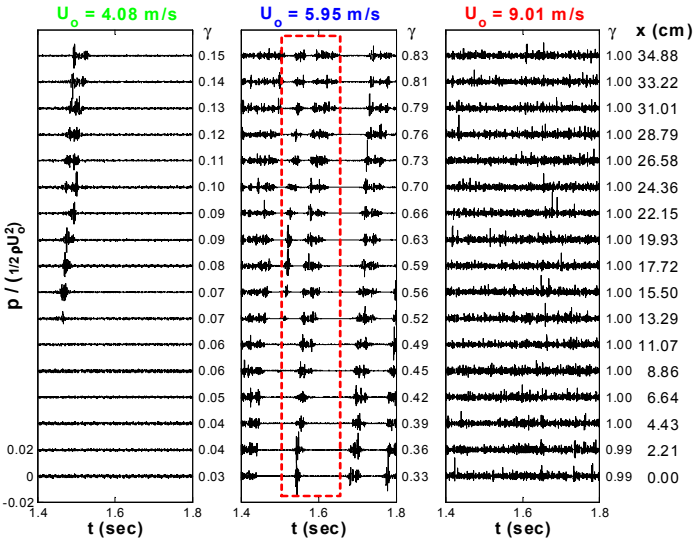

Figure 5. Time series across array (every 4th element) at U_o = 4.08, 5.95, 9.01 m/s.

this form, the spectra collapse indicating that the XBL spectrum is merely controlled by the fraction of time the field is in the turbulent state. This result has been presented previously in the literature [3, 4] and indicates that the spot turbulence is the same as that which exists in the fully turbulent boundary, at least to first order. Further evidence for this result has been provided by examining the spatial-temporal FFT of the full space-time array data or the wavenumber-frequency spectrum by Snarski [1] in which it was shown that the convective ridge spectral levels for the XBL and TBL collapse when scaled using an average intermittency level across the array. This previous result also validates some modeling work by Josserand and Lauchle [7] for the convective region ($k_c \sim \omega/u_c$) of the nonhomogeneous XBL wall pressure wavenumber-frequency spectrum.

The big remaining question, though, is WHAT ARE WE MISSING? Fourier transform based methods do not provide any spatial information and can not therefore tell us how the spectral content evolves with x. Although it is certainly possible to use windowed (short length) Fourier transforms over a reduced number of array elements where homogeneity can be assumed, the method offers little resolution with such a finite number of array elements. Furthermore, and perhaps more significant, Fourier transforms are intended for continuous processes not intermittent processes such as the XBL wall pressure field. Insight into what features of the field we may be missing can be revealed by considering the structure of the space-time XBL wall pressure field more closely. This is shown in Fig. 7 which is a contour plot of the portion of the U_o = 5.95 m/s time-series data set indicated by the red box in Fig. 5 but at all 64 array elements. In addition, Fig. 7 has been nondimensionalized via the outer length and time scales x/δ and tU_o/δ.

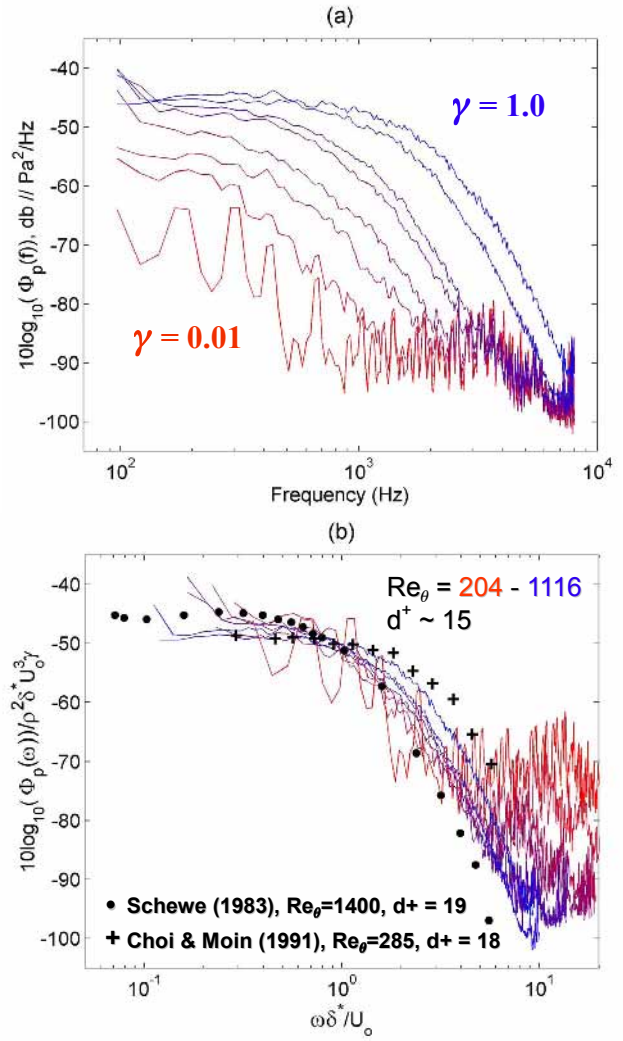

Figure 6. Wall pressure frequency autospectra at array center: (a) physical variables, (b) nondimensionalized.

Shown in Fig. 7 is the convection and evolution of two turbulent spots: one from the background unstable waves and the other captured shortly after formation through a largeportion of its development. Convection is evident by the inclination of the structure, while the spot growth is reflected by the divergence of the "turbulent wedge" with increasing x due to the differing convection velocities of the leading and trailing edges. The main point to extract from this figure is that two distinct length scales associated with the spot evolution process can be defined: (1) λ_c which characterizes the fluctuations *within the spots* due to convected turbulence, and (2) $\lambda_s(x)$ which characterizes *the spacing between the spots* and is controlled by the evolution dynamics of the spot structures (i.e., λ_S decreases monotonically with x, in an average statistical sense, as spots convect and grow). From Fig. 7, the convective turbulence within the spots scales with the boundary layer length scales (e.g., $\lambda_c \sim \delta$) consistent with the spectral results presented in Fig. 6. The length scales associated with the overall spot

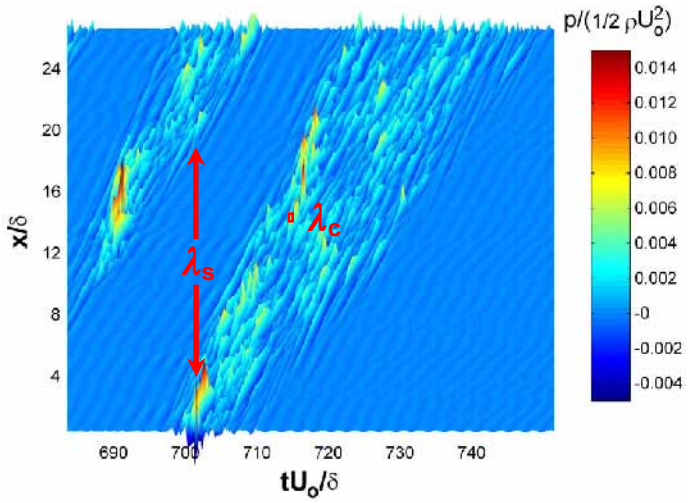

Figure 7. Wall pressure time series (all 64 elements) for region indicated by red box in Fig. 5.

evolution (spot spacing), on the other hand, are 1 to 2 orders of magnitude larger (e.g., $\lambda_s \sim$ 10-100δ) which is enormous compared to any length scale typically present in a TBL. Since all the turbulent activity is confined to the spot regions, $\lambda_s(x)$ defines the fundamental wavenumber $(1/\lambda_s)$ of turbulent wavepacket traveling pulse trains associated with the convecting spots. The obvious question is, What is the impact of these convecting pulses and very large length scale on the spectral character of the field?

To provide some insight into this question, the spectral energy content of three simple pulse train signals with different intermittency levels and hence fundamental pulse train frequencies is examined in Fig. 8. In these signals, a base sine wave of 100 Hz is used to represent the convective turbulence wavelength. The three intermittency levels of γ = 1.0, 0.5, and 0.1 are achieved by varying the pulse (spot) spacings or T_s = 0s, 0.085s, 0.262s, respectively. Beneath each signal is the Wavelet Transform (WT) time-frequency energy distribution, $E(f_a,t) = \pi\left|C(f_a,t)\right|^2$, where

$$C(f_a,t) = \frac{1}{\sqrt{a}}\int_0^T p(t')\psi\left(\frac{t-t'}{a}\right)dt' \quad , \qquad (1)$$

and $f_a = (\sigma/a)f_s$ with f_s = 2000 Hz (time series sampling frequency) and σ = 0.25 (db4 wavelet). In Fig. 8, red represents high magnitudes and blue represents low magnitudes.

Starting with the "fully turbulent" (γ = 1) signal in Fig. 8, the WT distribution clearly reveals the *continuous* periodicity in the signal at 100 Hz. For the intermittent signal with γ = 0.5, the *discontinuous* 100 Hz periodicity is effectively localized to just the energetic regions in time. In addition, the WT extracts the *continuous* energy associated with the pulse train periodicity as indicated by the concentration of energy at the fundamental

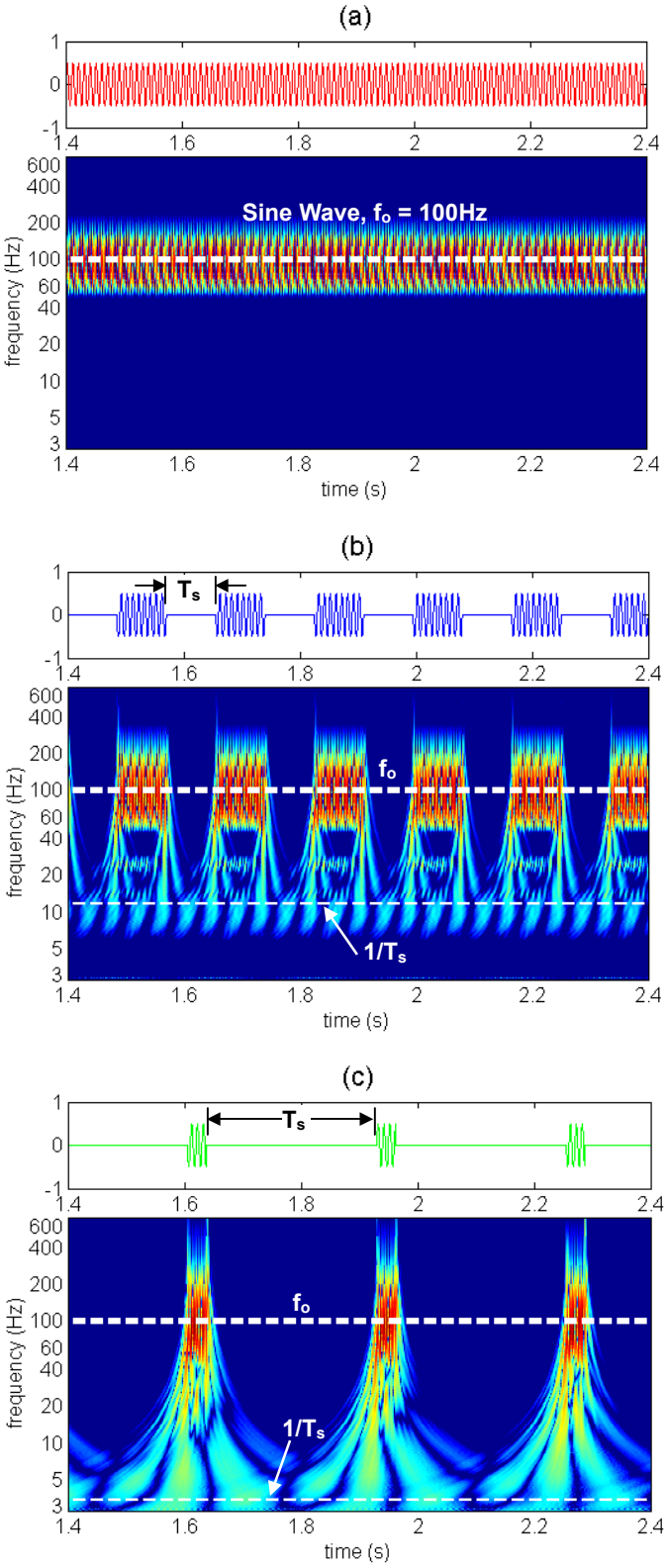

Figure 8. Wavelet transform time-frequency energy distributions (dB) for sinusoidal pulse train signals: (a) γ=1.0, (b) γ = 0.5 (T_s = 0.085s), (c) γ = 0.1 (T_s = 0.282s).

pulse frequency $1/T_s$ = 3.7 Hz at all times. For the intermittent signal with γ = 0.1, the same result exists except that the pulse energy has shifted to a lower frequency associated with the longer pulse period ($1/T_s$ = 11.8 Hz).

Although the result in Fig. 8 is insightful, a more quantitative comparison of the spectral characteristics can be obtained by evaluating the time integrated result or mean WT power spectrum for each signal [9], or

$$\mathrm{P}^*(f_a) = \frac{1}{\gamma T}\int_0^T E(f_a, t)dt \quad . \tag{2}$$

Equation (2) is normalized by the intermittency level γ consistent with the scaling used in Fig. 6. The results of Eq. (2) for the three test signals are shown in Fig. 9(a) along with the conventional FFT result in Fig. 9(b) given by

$$\Phi^*(f) = \frac{1}{\gamma}\left|\int_0^T p(\mathrm{t})\mathrm{e}^{-\mathrm{i}\omega t}\, dt\right|^2 \quad . \tag{3}$$

The WT results in Fig. 9(a) illustrate two interesting features. First, the spectra collapse in the 100 Hz "convective" region consistent with the wall pressure spectral result presented in Fig. 6(b). This simply illustrates that the root mean square energy level in each pulse ("turbulent spot") is the same for all three cases (same 100 Hz sine wave was used for all three cases). Second, the mean integrated WT spectra clearly reveal that in addition to a concentration of energy at low-frequencies in the domain of the fundamental pulse train frequency, there is a *systematic* shift of energy from low to high frequencies as the intermittency level increases. In Fig. 9(b), the superiority of the FFT for isolating tonal components in continuous signals is clearly revealed as evidenced by the 100Hz spike for the γ = 1 data. For the intermittent signals, however, although the low-frequency fundamental pulse train energy is present at the harmonics of $1/T_s$, the overall result is much more difficult to interpret.

The question at this point is whether the result demonstrated in Figs. 8 and 9 applies to the spatially nononhomogeneous intermittent convective XBL wall pressure field. Stated differently, does the intermittent nature of the XBL wall pressure field introduce energy at low wavenumbers and frequencies not present in the TBL? To answer this question, it is necessary to extend the one-dimensional sinusoidal pulse train formulation to the two-dimensional nonhomogeneous and intermittent random space-time field of the XBL wall pressure field. In the most direct sense, one could simply perform a two-dimensional WT of the form,

$$C(k_x, \omega, x, t) = \frac{1}{\sqrt{a_t a_x}}\int_0^L\int_0^T p(x', t')\,\psi\left(\frac{t'-t}{a_t}\right)\psi\left(\frac{x'-x}{a_x}\right) dt'dx' \,, \tag{4}$$

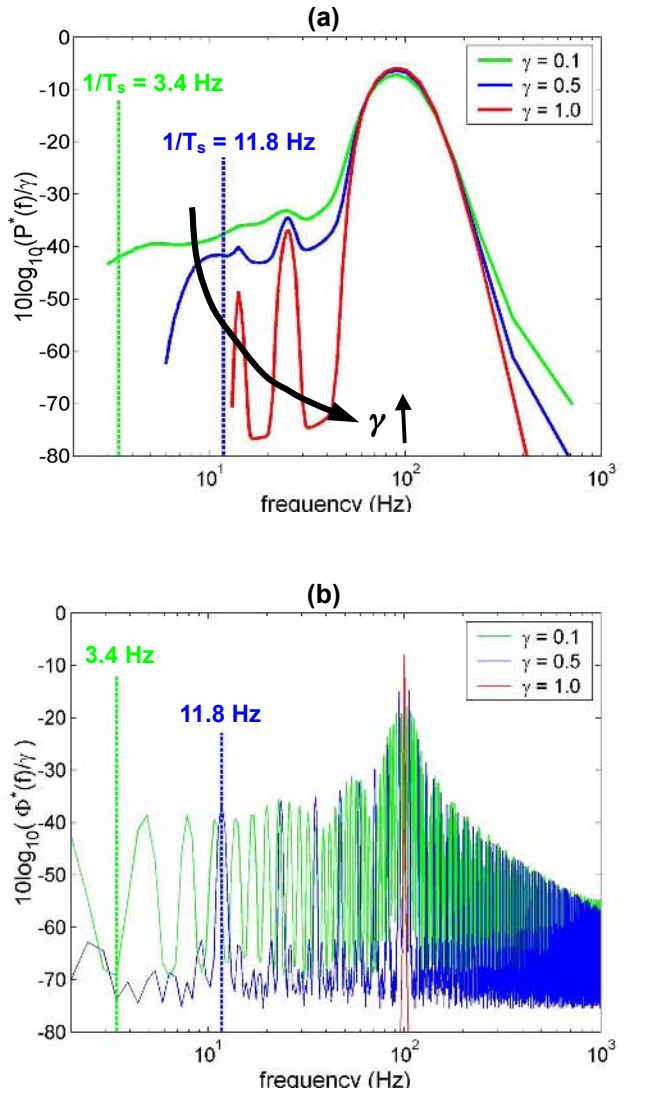

Figure 9. Frequency spectra for sinusoidal pulse train signals plotted in Fig. 8: (a) wavelet transform mean power spectra, (b) FFT spectra.

where $\omega \sim 2\pi / a_t$ and $k_x \sim 2\pi / a_x$. However, by considering the character of the XBL field, the required computational and memory resources can be greatly simplified. Examining the data in Fig. 5, although the XBL field is intermittent in both x and t, it is only nonhomogeneous in x. In time, the field is statistically stationary since the average temporal statistics are constant at any given spatial location. Consequently, it is possible to consider the space-varying frequency and wavenumber content of the XBL field *separately* through WT's in either time or space. In either case, the goal is to eliminate the stationary time variable which can be accomplished in either case by integrating in time.

The spatial and temporal WT mean power distributions can then defined by,

$$\mathrm{P}_t^*(f,x) = \frac{1}{\gamma(x)T}\int_0^T \pi \left|C_t(a_t,t;\ x)\right|^2\, dt \quad , \tag{5}$$

$$\mathrm{P}_x^*(k_x,x) = \frac{1}{T}\int_0^T \pi \left|C_x(a_x,x;\ t)\right|^2\, dt \quad , \tag{6}$$

where

$$C_t(a_t,t;\ x) = \frac{1}{\sqrt{a_t}}\int_0^T p(x,t')\,\psi\left(\frac{t'-t}{a_t}\right) dt' \quad , \tag{7}$$

$$C_x(a_x,x;\ t) = \frac{1}{\sqrt{a_x}}\int_0^L p(x',t)\psi\left(\frac{x'-x}{a_x}\right) dx' \quad . \tag{8}$$

The temporal integration in Eq. (5) for the temporal WT is equivalent to the integral operation in Eq. (2). The temporal integration in Eq. (6) for the spatial WT amounts to a statistical ensemble average over the whole time series equivalent to using a large number of sample records (averages) in an FFT analysis.

A preliminary result for the temporal WT given by Eq. (7) is shown in Fig. 10 for 3 second records of the U_o = 4.08, 5.95 and 9.01 m/s data at microphone 32 (γ = 0.08, 0.59, 1.0, respectively). The integrated result (Eq. 5 computed over 10.1 seconds of data) is shown in Fig. 11. Similar to the result for the sinusoidal pulse train signals in Fig. 8, the WT effectively localizes the convective energy from within the turbulent spots ($0.1 < \omega\delta^*/U_o < 10$) in Fig. 10. The integrated spectra also collapse reasonably well in this region ($1 < \omega\delta^*/U_o < 10$) in Fig. 11 indicating that the convective turbulence fluctuations within the XBL spots scale with the TBL fluctuations, consistent with Fig. 6(b). The low-frequency effect revealed in Figs. 8 and 9 for the sinusoidal pulse train, however, is not present for the XBL data in Figs. 10 and 11.

Examining the low-frequency portion of the WT spectra in Fig. 10 and 11, an increase in the spectral levels occurs below approximately 5 Hz for all three signals ($\omega\delta^*/U_o \sim 0.01 - 0.03$). It is suspected that this increase is an artifact of an inadequate record length used in the computation (T = 10.1 sec). Even so, the spreading effect seen towards low frequencies in Fig. 8 is not present in Fig. 9. This is likely because the XBL signal spot spacings are randomly distributed rather than constant as for the sinusoidal test signals such that there is not a discrete fundamental pulse frequency for the WT to isolate. Nevertheless, because the XBL spot spacings do have a quantifiable statistical mean ($\overline{T_s}$, $\overline{\lambda_s}$), one would expect that the wavepacket pulse trains should still produce a statistical distribution of energy about the mean fundamental frequency/wavenumber ($1/\overline{T_s}$, $1/\overline{\lambda_s}$). For the data in Fig. 10, the mean spacing is approximately $\overline{T_s}$ = 0.5s and 0.1s for the γ = 0.08 and 0.59 data, respectively, which corresponds to nondimensional frequencies of $\omega\delta^*/\mathrm{U_o}$ = 0.006 and 0.017,

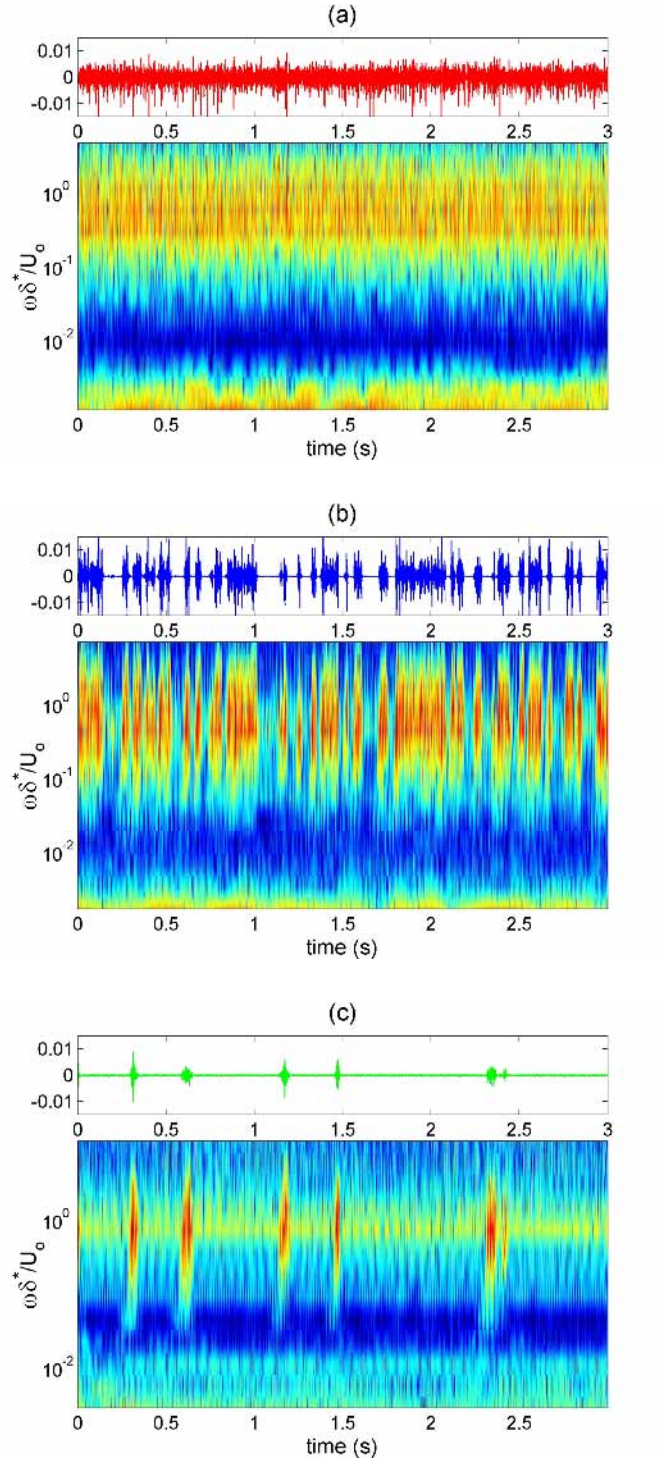

Figure10. Time series ($p(t)/\rho U_o^2$) and wavelet transform time-frequency energy distributions $E_t(f, t) = \pi|C_t(f, t)|^2$ (dB // $\rho^2\delta^* U_o^3\gamma$) for wall pressure signals at Mic 32: (a) U_o = 9.01 m/s (γ=1.0), (b) U_o=5.95 m/s (γ = 0.59), (c) U_o = 4.08 m/s (γ = 0.08).

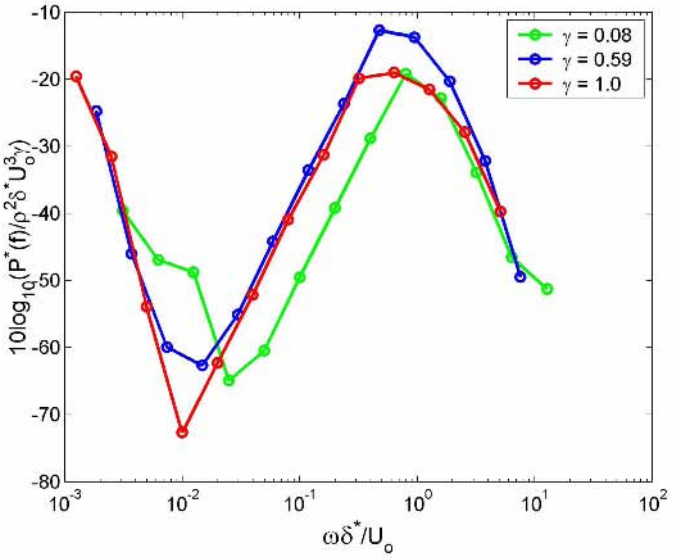

Figure11. Time-integrated mean wavelet transform frequency distribution for XBL data presented in Fig. 10.

respectively. Because these frequencies are within the corrupt portion of the WT spectra in Figs. 10 and 11, it is difficult to say whether or not any such effect is present. Even so, support for this pulse-train source of low-frequency (wavenumber) energy is provided from analyses of turbulent bursts in the fully developed TBL where the concept of a mean bursting period and associated frequency are well established (see for example Snarski & Lueptow [10]). Additional analyses are in progress to further interpret the apparently corrupt low-frequency WT spectral results in Figs. 10 and 11 and to further explore and quantify the potential wavepacket pulse-train source of low frequency (wavenumber) energy.

CONCLUSIONS AND FUTURE WORK

Measurements of the space-time fluctuating wall pressure field across the transition region of a flat plate zero pressure gradient boundary layer have been performed in an anechoic wind tunnel with a 64-element linear array of sub-miniature hearing-aid microphones (d^+ = 15). Wavelet transforms are being used to quantify the structure and nonhomogeneous wavenumber-frequency content of the field. The results illustrate that two disparate length/time scales must be considered when discussing the transitional boundary layer. The first, which characterizes the fluctuations *within the spots* due to the convected turbulence, scales with conventional boundary layer length scales. The second, which characterizes *the spacing between the spots* and is controlled by the evolution dynamics of the spot structures (turbulent spot wavepacket pulse trains), has a scale that is one to two orders of magnitude larger.

Consistent with previous findings, the structure and spectral

content of the fluctuations within the spots scale with the fluctuations which exist in a fully developed turbulent boundary layer. The influence of the convecting pulses and very large length/time scales associated with the turbulent spot wavepacket pulse trains on the spectral character of the field is less clear. It is conjectured here that since the turbulent spot spacings at any given location in the transition zone are randomly distributed about a quantifiable statistical mean ($\overline{T_s}$, $\overline{\lambda_s}$), the turbulent spot wavepacket pulse trains should produce a statistical distribution of energy about the associated mean fundamental pulse train frequency/wavenumber ($1/\overline{T_s}$, $1/\overline{\lambda_s}$). The concept was initially tested using sinsusoidal pulse train signals with various intermittency levels (mean spot spacings) where it was shown that the effect was quite strong. Wavelet transform analysis of the actual XBL data with spatio-temporal random spot distributions has not revealed the same effect. Nevertheless, support for the pulse-train source of low-frequency (wavenumber) energy is provided from published results of turbulent bursts in the fully developed TBL where the concept of a mean bursting period and associated frequency are well established.

Additional analyses using wavelet packets and discrete wavelet transforms with the complete space-time data set are planned to further interpret, quantify and explore the potential wavepacket pulse-train source of low frequency (wavenumber) energy and to examine the evolution of spectral components during spot formation and growth.

ACKNOWLEDGMENTS

This work was funded by the Naval Undersea Warfare Center In-house Laboratory Independent Research (ILIR) program and the Office of Naval Research (ONR 321SS). The author would like to give a special thanks to Dan Goldstein and Prof. Oleg Vasilyev of the University of Colorado and Prof. Kai Schneider of the University of Marseille for their expressed interest and helpful comments on this work during the APS-DFD 2002 meeting in Dallas, TX.

REFERENCES

[1] Snarski, S.R., 2002. "Measurement and Modeling of The Fluctuating Wall Pressure Field Beneath Transitional Boundary Layers," *ASME-Fluids Engineering Division, 2002 Summer Meeting*, Montreal, Quebec, Canada, July 14-18, 2002, FEDSM2002-31338.

[2] Cebeci, T. and J. Cousteix, *Modeling and Computation of Boundary-Layer Flows*, *Chapter 6: Transition in Two-Dimensional Flows*, Springer-Verlag, Horizons Publishing, Long Beach, CA, 1999.

[3] DeMetz, F.C., Farabee, T.M. and M.J. Cassarella, "Statistical Features of the Intermittent Surface Pressure Field in a Transitional Boundary Layer", in *Nonsteady Fluid Dynamics*, ed. D.E. Crow and J.A. Miller, ASME, 1978.

[4] Gedney, C.J. and P. Leehey, "Wall Pressure Fluctuations During Transition on a Flat Plate," in *Flow Induced Noise Due to Laminar-Turbulence Transition Process*, ed. T.M. Farabee, R.J. Hansen and R.F. Keltie, ASME NCA-Vol. 5, pp. 1-10, 1989.

[5] Gedney, C.J. and P. Leehey, 1984, *Measurements of the Low Wavenumber Wall Pressure Spectral Density During Transition on a Flat Plate*, TR 93019-1, Acoust. Vib Lab, MIT Cambridge, MA.

[6] Audet, J., Dufourq, Ph., and M. Lagier , "Fluctuating wall pressures under a boundary layer during the translation to turbulence," *J. Acousticue* [French], Vol. 2, pp. 369, 1989. [see translation by Marboe, R.C., ARL Penn State, TM 91-81, 5 Apr 1991].

[7] Josserand, M. and G.C. Lauchle, "Modeling the Wavevector-Frequency Spectrum of Boundary-Layer Wall Pressure During Transition on a Flat Plate," *ASME J. Vib. And Acous.*, Vol. 112, pp. 523-534, 1990.

[8] Lauchle, G.C. and S. Park, 2000, *Low-Wavenumber Wall Pressure Fluctuations due to Boundary-Layer Transition*, Applied Research Laboratory, TM 00-100, State College, PA.

[9] Jaques Lewall, *Tutorial on Continuos Wavelet Analysis of Experimental Data*, Syracuse Univ., Syracuse, NY, April 1995, www.mame.syr.edu/faculty/lewalle/tutor/tutor.html.

[10] Snarski, S.R. and R.M. Lueptow, "Wall Pressure and Coherent Structures in a Turbulent Boundary Layer on a Cylinder in Axial Flow," *Journal of Fluid Mechanics*, Vol. 286, pp. 137-171, 1995.